Issues Associated With Polarization Independence in Silicon Photonics

Graham T. Reed, Goran Z. Mashanovich, William R. Headley, Branislav Timotijevic, Frederic Y. Gardes, Seong Phun Chan, Peter Waugh, Neil G. Emerson, Ching Eng Png, Mario J. Paniccia, *Senior Member, IEEE*, Ansheng Liu, Dani Hak, and Vittorio M. N. Passaro, *Senior Member, IEEE*

(Invited Paper)

***Abstract*—Interest in silicon photonics is experiencing a dramatic increase due to emerging applications areas and several high profile successes in device and technology development. Despite early work dating back to the mid-1980s, dramatic progress has been made only in the recent years. While many approaches to research have been developed, the striking difference between the work of the early to mid-1990s, and more recent work, is that the latter has been associated with a trend to reduce the cross sectional dimensions of the waveguides that form the devices. The question arises therefore, as to whether one should move to very small strip waveguides (silicon wires) of the order of 250 nm in height and a few hundred nanometres in width for improved device performance but with little hope of polarization independence, or to utilize slightly larger rib waveguides that offer more opportunity to control the polarization dependence of the devices. In this paper, we discuss the devices suitable for one approach or the other, and present the designs associated both with strip and rib waveguides. In particular, we present the designs of polarization-independent ring resonators with free spectral ranges up to 12 nm, we propose modulators for bandwidths in the tens of gigahertz regime, and present grating-based couplers for rib and strip waveguides, and/or for wafer scale testing, as well as a novel means of developing Bragg gratings via ion implantation.**

***Index Terms*—Bragg gratings, grating couplers, optical modulators, polarization independence, rib waveguides, ring resonators, silicon-on-insulator (SOI), single-mode condition.**

I. Introduction

Silicon photonics is a research field that is surprisingly mature in some senses, having been studied since the mid-1980s. In other ways, it is in its infancy, with some major advances being reported only very recently. The first waveguides were reported in the mid-1980s, in silicon on doped silicon [1], silicon on sapphire [2], silicon germanium [3], and silicon on insulator (SOI) [4], [5]. The SOI platform, first reported in 1989, has by far become the most popular of the four waveguide systems that has formed the core of the work carried out by the Silicon Photonics Group at the University of Surrey, Guildford, U.K., which was established in 1989. The first results from the group were published in early 1991, demonstrating the waveguides formed by the SIMOX process [6]. These early waveguides exhibited losses as high as 30 dB/cm, but within a year the same group had reported waveguides with a loss of less than 1 dB/cm, demonstrating the viability of the technology [7].

The first silicon-based optical modulators were proposed in 1986, with modeling suggesting that a π-radian phase shift could be achieved in a device less than 1-mm long. The corresponding loss was less than 1 dB at $\lambda = 1.3\ \mu$m for both the TE and TM polarizations [8]. However, the electrical power densities required to drive the early modulators were very high, and it was not until 1993 that the Surrey group proposed a three-terminal device, which reduced the power consumption by an order of magnitude [9], [10]. The device variants had bandwidths of up to 20 MHz, and were based upon a waveguide with large cross-sectional dimensions of the order of 6 μm, and a drive current of only 7 mA [11]. Nevertheless, more recent work has proposed and/or demonstrated fast modulators in smaller waveguides, with drive currents below 1 mA. Some of these devices will be discussed later, together with our other work on ring resonators, grating-based devices, and optical couplers. First, however, let us consider some fundamental issues associated with the shrinking of the waveguide cross-sectional dimensions.

II. Fundamental Waveguide Issues

Single-mode SOI rib waveguides with large cross section, have been studied extensively by a number of researchers [12]–[17] to find single-mode behavior at the same time as the low propagation loss. The majority of these photonic devices in SOI have been studied in waveguides that are multimicron in cross-sectional dimensions (to the order of 5 μm), to facilitate low-loss coupling to and from the optical fibers. Soref *et al.* [13] first proposed a simple expression for these large rib waveguides, related to their geometry to ensure that they satisfy the single-mode condition (SMC)

$$\frac{\mathrm{W}}{H} \leq \alpha + \frac{r}{\sqrt{1-r^2}}, \qquad \text{for} \quad 0.5 \leq r \leq 1 \qquad (1)$$

Manuscript received October 26, 2005; revised August 9, 2006. This work was supported in part by the Engineering and Physical Sciences Research Council, U.K., in part by Bookham Technology Inc., U.K., in part by Intel Corporation, USA, in part by Agilent Technologies, Singapore, and in part by the University of Surrey, Guildford, U.K.

G. T. Reed, G. Z. Mashanovich, W. R. Headley, B. Timotijevic, F.Y. Gardes, S. P. Chan, P. Waugh, and N. G. Emerson are with the Advanced Technology Institute, School of Electronics and Physical Sciences, University of Surrey, Guildford GU2 7XH, U.K. (e-mail: g.reed@surrey.ac.uk).

C. E. Png is with the Institute of High Performance Computing, Singapore 117528.

M. J. Paniccia and A. Liu are with Intel Corporation, Santa Clara, CA 95054 USA.

D. Hak is with Intel Corporation, Jerusalem 91031, Israel.

V. M. N. Passaro is with the Dipartimento di Elettrotecnica ed Elettronica, Politecnico di Bari, 70125 Bari, Italy.

Digital Object Identifier 10.1109/JSTQE.2006.883136

where r is the ratio of the slab height to the overall rib height, W/H is the ratio of the waveguide width to the overall rib height, and $\alpha = 0.3$. The analysis of the waveguides was limited to the shallow-etched ribs $(r > 0.5)$, and hence, deeply etched rib waveguides were not considered. Furthermore, the waveguide dimensions were assumed to be larger than the operating wavelength. Their analysis was based on the assumption that high-order vertical modes (i.e., modes other than the fundamental mode) confined under the rib waveguides, were coupled to the outer slab region during propagation, thereby yielding high propagation losses for the higher order modes. Thus, the waveguides behave as single-mode waveguides, as all other modes are lost. Other authors have also considered the single mode for large waveguides, and produced similar expressions (e.g., [14], [15]). However, the current trend in silicon photonic circuits to move toward smaller device dimensions for improved cost efficiency and device performance can come at some cost to other performance parameters, notably in the polarization dependence of the circuits, if they are not carefully designed. Furthermore, Soref's design equation given in (1) cannot be applied to small and deeply etched rib waveguides. In order to maintain the consistency with other work [13], [15]–[17], we have used the full-vectorial beam propagation method (BPM)[1] to analyze the deeply etched rib waveguide structure, mode propagation within it, and polarization independence. Some results of the SMC condition have also been verified by the finite-element method (FEM).[2] For rib waveguides, we have evaluated the single mode cutoff condition by determining when the first mode of a higher order than the fundamental mode begins to propagate. Because the waveguides are relatively small, for high etch depths $(r < 0.5)$, the single-mode condition becomes dominated by the boundary conditions, and hence, the conditions for quasi-TE and quasi-TM modes begin to diverge. We have also determined the difference between the effective indices of the fundamental mode as a function of waveguide width and etch depth (parameter r defined above), for a given waveguide height. The condition when the effective indices are equal is defined as the zero-birefringence condition, and there are up to two such events for each waveguide etch depth. By determining these conditions, we can plot a "zero-birefringence locus" for each waveguide height [18].

The simulations were carried out for rib waveguides of silicon $(n_g = 3.477)$ on silica $(n_s = 1.444)$ and an upper cladding, that is air $(n_c = 1)$, although it is a simple task to extend the work to an upper oxide cladding. SOI rib waveguides with an overall height H in the range 1.00–1.50 μm were analyzed at a wavelength of 1.55 μm. Both the single-mode and the zero-birefringence conditions can be conveniently plotted on the same curve to determine the waveguide parameters that allow both the conditions to be satisfied simultaneously. For example, Fig. 1 shows such plots for waveguide heights of 1.35 μm [Fig. 1(a)] and 1.5 μm [Fig. 1(b)]. It can be seen from Fig. 1 that for truly single-mode behavior, it is the quasi-TM condition that is the limiting condition, because if this is satisfied, then the

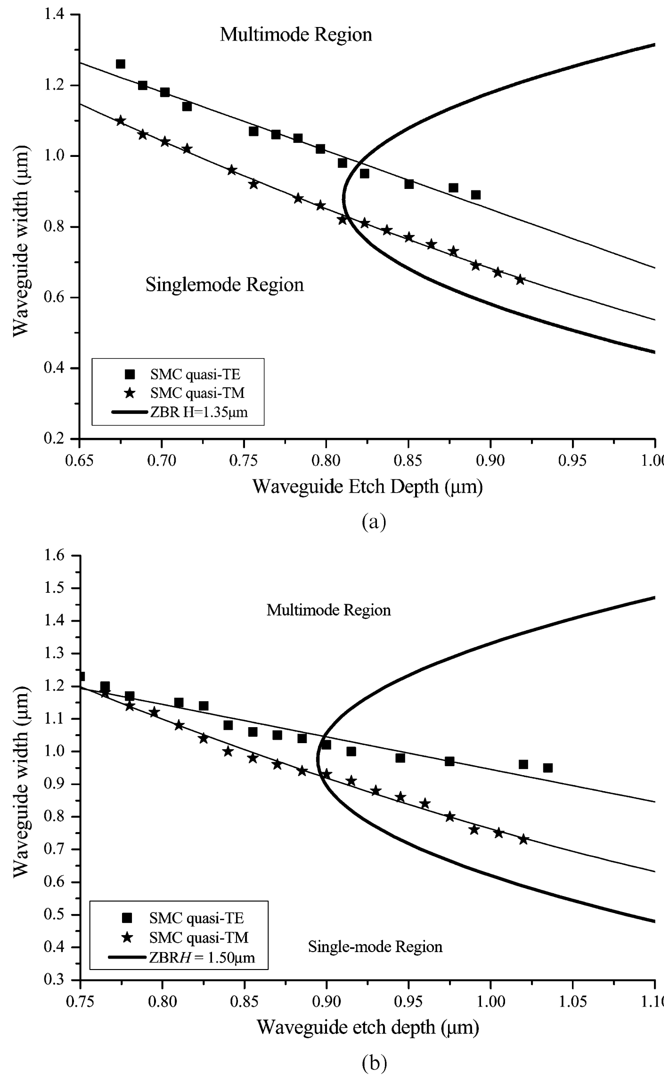

Fig. 1. Single-mode condition and the zero birefringence condition for a rib waveguide with height H. (a) $H = 1.35\,\mu$m. (b) $H = 1.5\,\mu$m.

quasi-TE condition is automatically satisfied. Consequently, for both single-mode behavior and polarization independence, the waveguide design should lie on the zero-birefringence locus, below the quasi-TM single-mode boundary, in the bottom right-hand corner of Fig. 1(a) and (b). From this and other data [18], [19], we can extract design rules to aid the design of single-mode rib waveguides, for waveguide heights H in the range 1.00–1.50 μm

$$\frac{W}{H} \le 0.05 + \frac{(0.94 + 0.25H)r}{\sqrt{1 - r^2}}, \quad \text{for } r \le 0.5 \text{ and } 1.0 \le H \le 1.5 \tag{2}$$

$$D_{\min} = 0.06 \times 10^{-6} + 0.556H. \tag{3}$$

The quasi-TM single-mode boundary is defined in (2), and hence provides guidance on the geometric limitations to retain

[1]BeamPROP by RSoft Design Group, Inc., Ossining, NY.
[2]FEMLAB by COMSOL Inc., Burlington, MA.

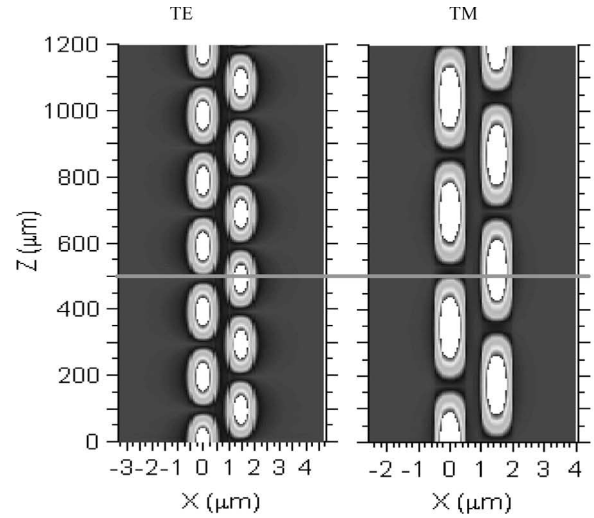

(a)

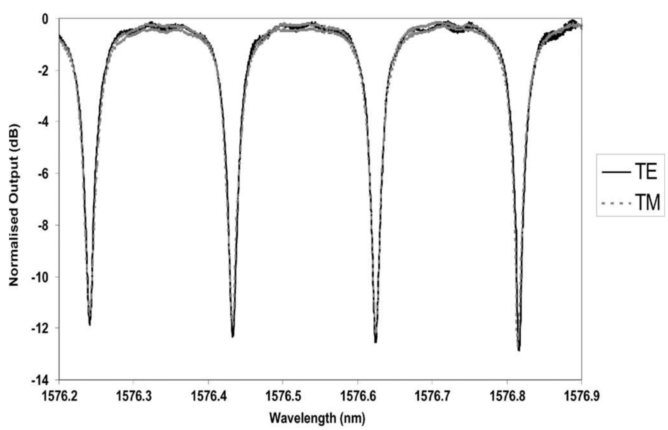

(b)

Fig. 2. (a) Modeling of a directional coupler to show polarization-independent transfer of power from the left waveguide to the right waveguide, for a coupling length of 500 μm. (b) Measured spectral response of a polarization-independent racetrack resonator.

single-mode behavior, whilst (3) defines the minimum etch depth required to obtain polarization independence.

III. Ring Resonators in Rib Waveguides

We can utilize the information in Section II to design a polarization independent ring resonator. Such a resonator not only requires polarization-independent waveguides for the matching of TE/TM phase shifts around the ring waveguides, but also requires polarization-independent directional couplers to transfer the light to and from the ring. A directional coupler (DC) comprises two waveguides in close proximity such that the evanescent fields of the optical modes overlap, and light can transfer from one waveguide to the other. We have previously described how to design such a coupler [20] by allowing multiple passes of light from one of the waveguides in the DC to the other. For example, Fig. 2(a) shows modeling of the optical power in the two arms of a directional coupler. For the purposes of the modeling, the left arm of the coupler was excited with an optical field. With a propagation distance z, light transfers from the left waveguide to the right, and back again in a cyclic manner. The goal of modeling is to find a coupler length that yields the same degree of power transfer from the left waveguide to the right, for both polarizations.

TABLE I
Comparison of the FSR Achieved for Ring Resonators Fabricated With Varying Circumference

Bend Radius	Total circumference	FSR	Q
400μm	3513μm	0.193nm	90,000
300μm	2505μm	0.251nm	170,000
200μm	1877μm	0.333nm	30,000
50μm	934μm	0.691nm	30,000
25μm	777μm	0.815nm	19,200

Fig. 2(a) demonstrates that power transfers in a shorter length for the TE polarization than for the TM. However, for the three transitions of the TM mode and five transitions of the TE mode, the power in the left waveguide has transferred to the right waveguide, over a coupler length of approximately 500 μm, and hence, for this fixed coupling length the device is polarization independent. A ring resonator utilizing this principle was fabricated, and the experimental characteristics are shown in Fig. 2(b), which clearly demonstrates a polarization-independent performance over a spectral width of three times the free spectral range (FSR). This device was based upon a waveguide height of 1.35 μm and a rib width of 0.8 μm.

However, the resultant FSR is very small, due to the relatively large circumference of the ring resonator, which in turn is a direct result of the size of the waveguides. Consequently, it could be argued that resonators based on strip waveguides would be more useful, as the ring circumference could be much smaller (~ 5 μm) leading to FSRs to the order of 10–20 nm (e.g., [21]). However, we can push the large ring resonators further, either by simply shrinking the ring circumference, or by employing the cascaded or multiple ring resonators. Let us first consider shrinking the ring circumference. The device resulting in the data of Fig. 2(b) had a bend radius of 400 μm and a total circumference of 3513 μm, resulting in an FSR of only 193 pm. We have also fabricated a series of other resonators with varying circumference, based on identical waveguide dimensions. The results of these devices are summarized in Table I. This table shows that if the bend radius is reduced to 25 μm, the FSR can be increased significantly to 815 pm. However, this is still very small for many applications. Consequently, we can investigate both the cascaded resonators and devices based on the serial coupling of multiple rings.

We have carried out the modeling of both such devices based on the experimental results summarized in Table I. For example, if we consider the cascaded ring resonators based on our devices with a bend radii of 25 and 50 μm, the data of Fig. 3(a) results

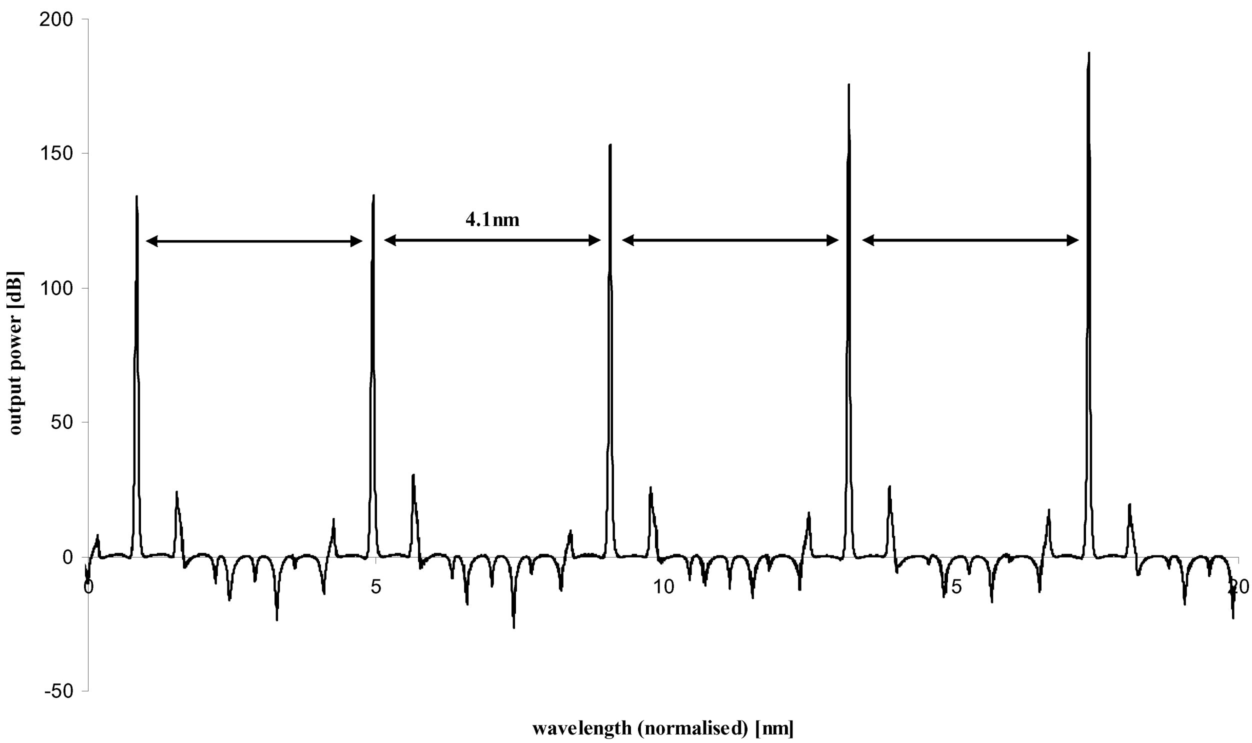

(a)

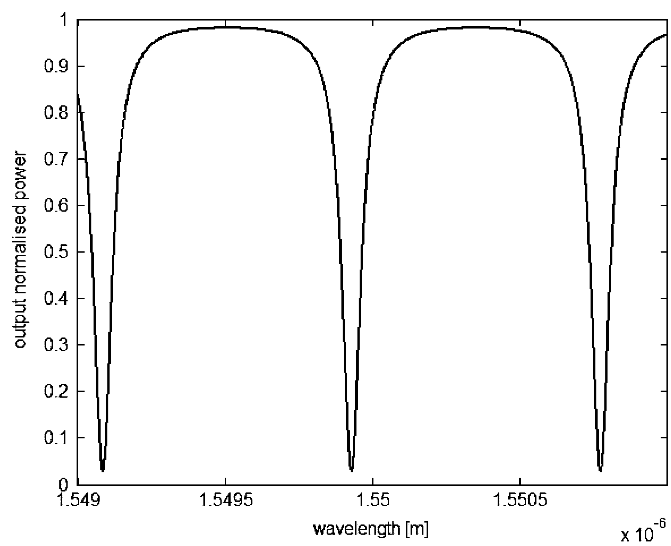

(b)

Fig. 3. Modeled response of (a) cascaded ring resonators and (b) serially coupled double-ring resonators based upon experimentally measured devices with bend radii of 25 and 50 μm, a coupler length of 500 μm, and waveguide height of 1.35 μm.

exhibit an FSR of approximately 4.1 nm. In such a configuration, light propagates through the first resonator, straight section, and finally through the second resonator toward the output drop port. If the rings are different, the resonant conditions are different, and only those wavelengths that satisfy both of them will be present at the output. Therefore, the device acts as an "and" function between the two rings and the net transfer function [Fig. 3(a)], and can be approximated by multiplying the responses of single racetrack resonators employing 310-μm couplers and bend radii of 25 and 50 μm assuming the same coupling and propagation conditions as for the single stage filters. Alternatively, a device with serially coupled rings of radii of 25 and 33.24 μm and with the length of the coupler of 310 μm, exhibits the so-called Vernier effect with a much improved FSR of approximately 12 nm. The value for the second radius has also been obtained by observing single-stage filter response for a 25-μm racetrack, assuming the same coupling conditions and taking into account the Vernier condition $m \times \mathrm{FSR}_1 = n \times \mathrm{FSR}_2$ [22]. By choosing these values for bend radii and the length of the coupler, the total FSR becomes 15 times

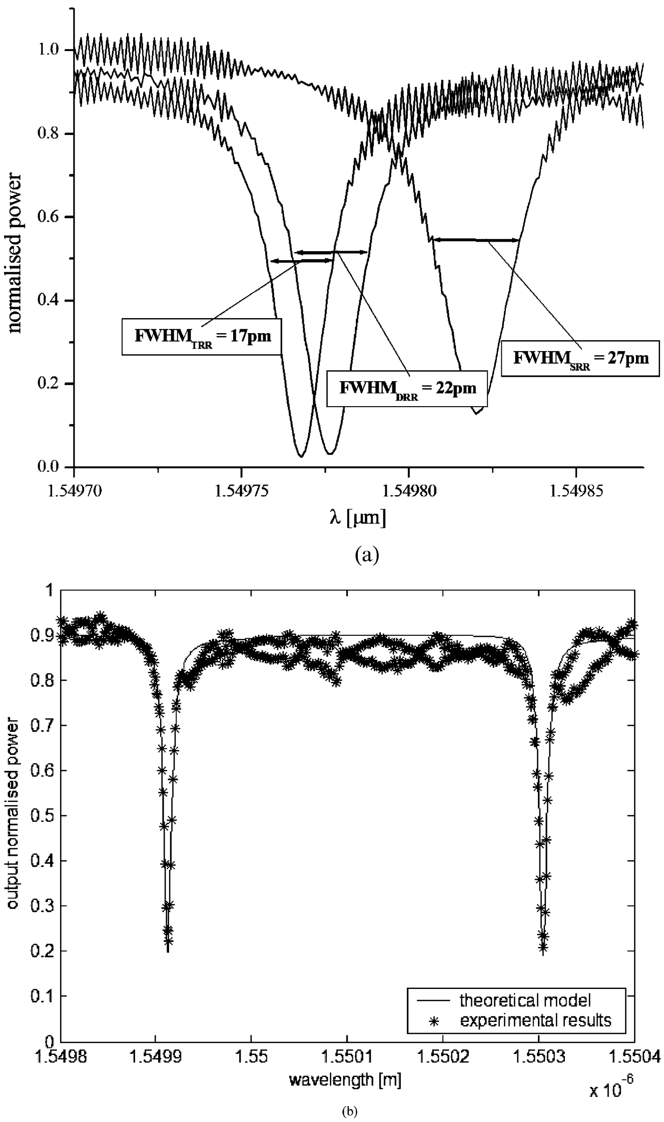

Fig. 4. (a) Measured FWHMs of a triple-ring resonator (TRR), a double-ring resonator (DRR), and a single-ring resonator (SRR) with similar serially coupled rings are 17, 22, and 27 pm, respectively. (b) Theoretical and measured responses of the DRR with similar rings.

bigger than the FSR for the 25-μm single ring, the spectrum of which is given in [Fig. 3(b)], but it should be also noted that this design requires a very careful matching of the coupling coefficients and, consequently, a control of fabrication issues. This figure could be improved further by reducing the coupler length and, hence, the circumference, by using the MMI couplers. Nevertheless, it is clear that the FSRs are possible in polarization-independent resonators that approach the FSR performance of very small ring resonators, which would almost certainly be highly polarization dependent.

It is worth considering one further improvement of the multiple-ringed resonator structure. By serially coupling the similar rings (rather than dissimilar rings for FSR improvement), we can vary the full width at half maximum (FWHM) of the resonance, and hence change the effective Q factor of the device. For example, Fig. 4 shows the experimental results of the ring resonator devices with single-, double-, and triple-ringed devices, each with rings of the same size. The devices were based on the same waveguides as previously, and a directional coupler of 2010 μm, resulting in a FWHM of 27 pm for a single-ring device, 22 pm for a dual-ring device, and 17 pm for a triple-ring device. Fig. 4(b) shows that the experimental results of a double-ring resonator compares extremely well with the theoretical transfer function, demonstrating that we have excellent control over the design parameters of such devices.

IV. Grating-Based Devices

Gratings have numerous applications in optical circuits including filtering, coupling to/from circuits, and phase matching in directional couplers, and as Bragg reflectors. Since a grating is a highly polarization dependent device, its application in the polarization independent waveguides is questionable. However, if the grating can be made to respond only to one polarization, then cascading two gratings can result in a device that is effectively polarization independent. A Bragg reflector is an obvious example of such a device.

We have carried out grating work in silicon waveguides ranging in height from 1 to 1.5 μm. Our earliest work dates back to 1998, and was based on grating couplers for input/output coupling. Fig. 5 shows grating couplers on the surface of 1-μm waveguides. Fig. 5(a) shows a conventional castellated grating that exhibited a measured out-coupling efficiency of 72% at a wavelength of 1.3 μm [23], and Fig. 5(b) shows a blazed grating, also on a 1-μm waveguide that exhibited an increased out-coupling efficiency of 84% at a wavelength of 1.3 μm [24]. Such gratings are useful for laboratory-based coupling experiments, but may also have much wider application in wafer scale testing of the silicon photonic circuits.

We are now working on similar gratings, as well as Bragg gratings that can be formed by an ion implantation of oxygen, or other species. The advantage of such an approach is that there is no physical etch of the waveguide surface, and the planar surface retention is easier to process. Furthermore, it is more convenient to integrate them with other devices, such as heaters, to enable thermal tuning of the gratings, or perhaps with electronics. The development of gratings fabricated via ion implantation relies on a modification of the refractive index at the waveguide surface in a periodic manner. This can be achieved in silicon by ion implantation through a mask, and hence, the design is critically dependent upon achieving good control of the surface implant. Thus, modeling of the surface implant as well as the required subsequent annealing process is important. Grating depths up to 150 nm are being considered. Oxygen is a good choice for the implant, as the annealing process results in a definitive interface between the silicon dioxide resulting from the oxygen implant, and the remaining surface silicon, similar to the work reported by Bussman *et al.* [25]. Fig. 6 shows the predicted implant profile of 30 keV oxygen into silicon. Clearly, the implant is not truly a surface implant, but the subsequent annealing process results in the diffusion of oxygen into a near-stoichiometric surface layer of SiO_2.

The preceding examples of the grating structures are compatible with the rib waveguides to the order of 1–2 μm in height.

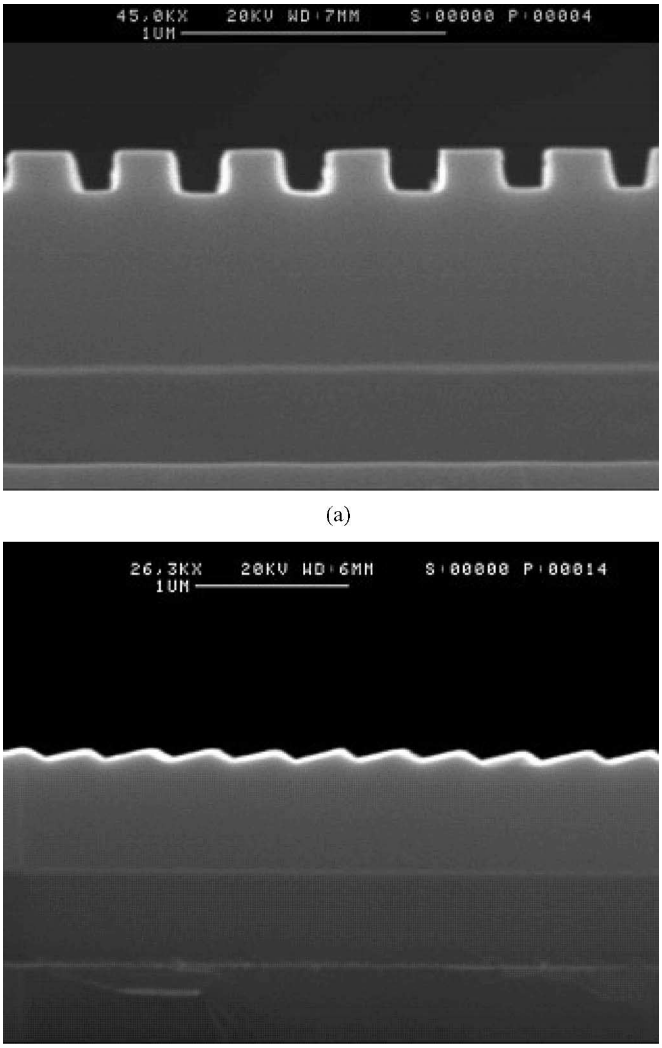

Fig. 5. (a) Cross section of a castellated surface grating coupler fabricated on a 1-μm silicon waveguide. The period is approximately 400 nm, designed to operate at $\lambda = 1.3\,\mu$m, and the output efficiency was 72%. (b) Cross section of a blazed surface grating coupler fabricated on a 1-μm silicon waveguide. The period is approximately 383 nm, designed to operate at $\lambda = 1.3\,\mu$m, and the output efficiency was 84%.

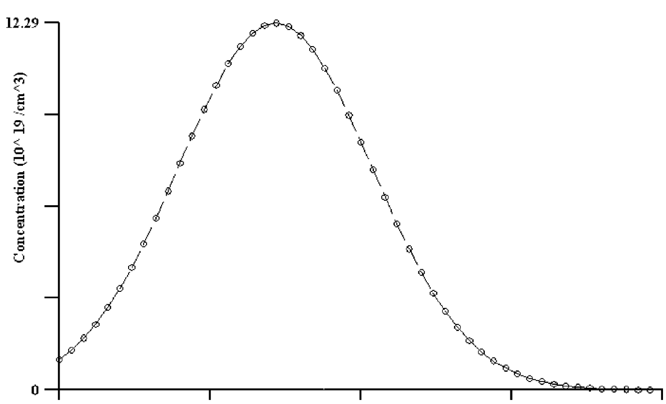

Fig. 6. Simulation of 30 keV oxygen ions implanted into the surface of a silicon waveguide, showing the implanted profile and ion-induced damage prior to annealing.

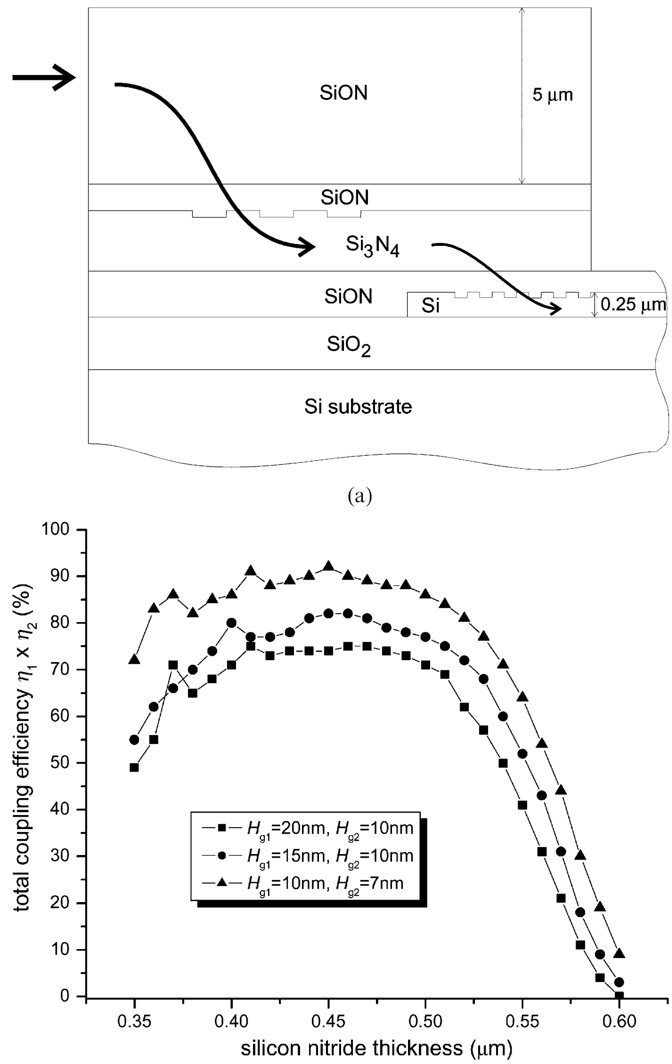

Fig. 7. (a) Cross-sectional view of a DGADC, to couple light from an optical fiber to a small silicon waveguide. (b) Predicted efficiency of the DGADC depicted in Fig. 7(a) for a range of combinations of grating heights.

However, we have built upon our work on surface gratings to develop a coupler device for coupling into very small waveguides, such as silicon wires, for applications in which polarization independence is less important. We have developed a device, which we have entitled as the dual grating assisted directional coupler (DGADC) [26].

A DGADC in SOI is shown in Fig. 7(a) [26]. A thick waveguide and two separation layers are fabricated in SiON for refractive index control over a broad range (1.45–2). The top layer is 5-μm thick with the refractive index close to the refractive index of optical fiber, resulting in an insertion loss of ≤ 0.05 dB from the fiber to this first waveguide.

A fiber is butt-coupled to the thick SiON waveguide, and subsequently, the light is coupled to an Si_3N_4 waveguide using the first grating, and to the thin ($\approx 1/4\mu$m) SOI waveguide via the second grating. The Si_3N_4 waveguide is crucial for the operation of the device, because it enables highly efficient coupling at both the gratings, consequently forming an efficient

DGADC. This waveguide bridges the gap between the SiON and Si layers in both refractive index and thickness. The buried oxide layer serves as the lower cladding layer, for isolation from the substrate, and hence removes any leakage loss toward the substrate. Fig. 7(b) shows the theoretical efficiency of the structure achieved via modeling. The total efficiency is expressed as the product of the efficiencies of the first grating (η_1) and the second grating (η_2), as a function of the thickness of the Si_3N_4. The efficiency is plotted for three different combinations of grating heights. The most important point to note from this graph is that the theoretical coupling efficiency can exceed 90%. We have yet to fabricate the optimum device, but we have recently reported the preliminary results measured for a device with a surface waveguide height of $\sim 3.7\mu$m, which in turn means that the theoretical coupling is 60% [27], rather than >90% in the optimized device. However, the experimentally determined efficiency was 55%, very close to the theoretical value. This is already a competitive performance for coupling to such small waveguides, but perhaps more importantly, this result means that the DGADC remains amongst the most promising devices for very high efficiency coupling to very small waveguides. The measured bandwidth of ~5 nm can be broadened significantly by chirping and by varying the duty cycle of the gratings.

V. Modulators for Rib and Strip Waveguides

Owing to the fact that fast modulators in silicon must probably be realized via the plasma dispersion effect, the modulators will always be faster and more efficient in a smaller waveguide as compared to a similar modulator in a larger waveguide. However, one of the fastest modulators reported to date has been fabricated in a rib waveguide [28]. Therefore, both rib and strip waveguides are worthy of consideration.

In 2003–2004, we reported the simulation of a p-i-n modulator based on a rib waveguide with an overall waveguide height of approximately 1 μm [29], [30]. The structure is shown in Fig. 8(a). The doping profile of the n^+ regions was optimized to provide maximum modulation speed. This optimum doping profile in the side n^+ regions was achieved through the modeling of a series of different implantation steps, such that the peak concentration at the surface of the n^+ contact was approximately $10^{20}\mathrm{cm}^{-3}$ and decreased to approximately $10^{16}\mathrm{cm}^{-3}$ at the interface between the silicon and the buried oxide. The determination of this profile was achieved through the process simulation package, ATHENA from Silvaco.[3] The optimum profile predicted a current requirement to achieve a phase modulation of π radians, $\boldsymbol{I}_\pi$ of 0.7 mA, as well as rise and fall times of 0.38 and 0.13 ns, respectively, corresponding to a device bandwidth to the order of 1 GHz. We also showed that by overdriving, the rise and fall times of the modulator can be further improved to provide a bandwidth in excess of 5 GHz, an effect that has since been used by Xu *et al.* [31] to overdrive a ring resonator modulator in a strip waveguide to achieve a data rate of 1.5 Gb/s.

We have recently reported the modeling of a faster modulator suitable for width dimensions similar to those of a strip waveguide [32]. This device is shown in Fig. 8(b). It is fabricated in a waveguide that, whilst having dimensions approaching those of silicon wire dimensions, is technically still a rib waveguide and, hence, some polarization control is still possible. The device has an asymmetrical pn structure, where two slab regions are joined as a common cathode, and two polysilicon regions are joined as a common anode. Both n^+ and p^+ regions were modeled as highly doped regions with peak doping concentrations of $1 \times 10^{19}\mathrm{cm}^{-3}$. The structure is based around an overall silicon thickness of 0.45 μm, etched rib waveguides 0.415-μm wide with a slab thickness of 0.1 μm. These dimensions were chosen to approach the polarization independence operational regime. The silicon slab and the bottom part of the rib have an n-type background doping concentration of $4 \times 10^{17}\mathrm{cm}^{-3}$, and the top part of the rib has a p-type background doping concentration of $2 \times 10^{17}\mathrm{cm}^{-3}$. The n^+ doped regions are situated on both sides of the wave guiding region in the slab, 1.5 μm from the center of the waveguide. Furthermore, the polysilicon p^+ doped regions are situated on both sides of the top of the rib in order to reduce the losses resulting from the polysilicon and aluminium contacts.

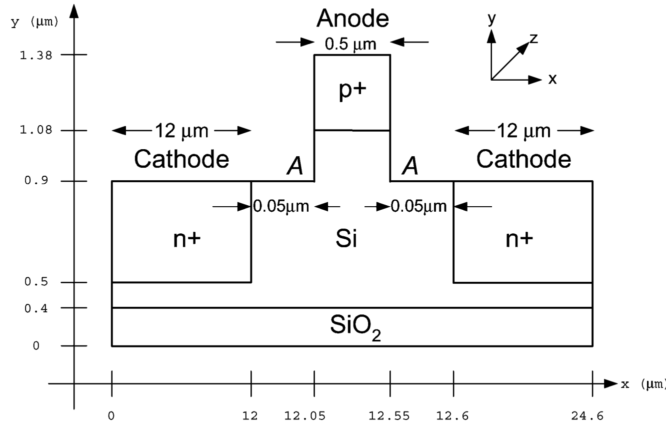

(a)

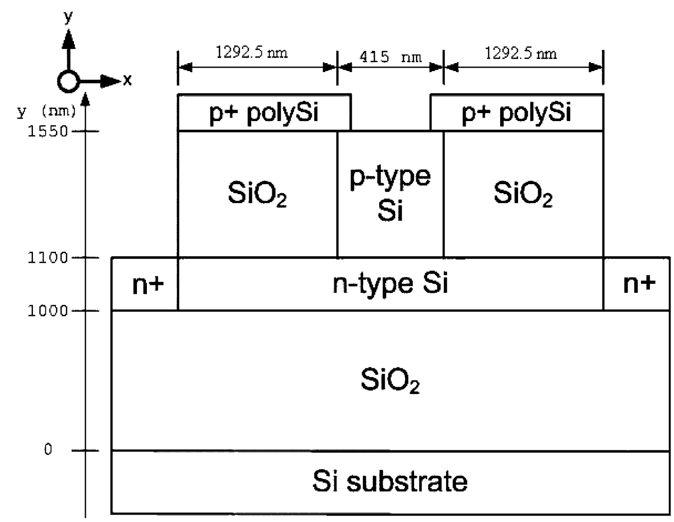

(b)

Fig. 8. (a) Cross-sectional view of a p-i-n phase modulator, designed for operation in a 0.98-μm height rib waveguide. (b) Cross-sectional view of a depletion modulator for inclusion in a push–pull Mach–Zehnder interferometer.

[3]Silvaco International, Santa Clara, CA.

The modulation mechanism was carrier depletion from the pn junction. Carrier losses induced were minimized in our design. Modulation was proposed by including two devices in a Mach–Zehnder interferometer, to operate in the push–pull mode. In the "off" state, both devices were reverse biased to 5 V, such that no phase difference was induced between the arms of the Mach–Zehnder interferometer. In the "on" state, one arm was reverse biased to 10 V, whilst the bias on the other was reduced to 0 V, to induce a π radian phase shift between the arms. The transient time of each device was characterized by ATLAS [3] in terms of carrier concentration against time. The carrier concentration profile for a reverse bias of 5 V was taken as a reference. The change in carrier concentration compared to a reverse bias of 5 V (against time) was converted to a change in refractive index profile (against time). This profile was then used in BeamPROP [1] simulation to determine the change in effective index, which was subsequently converted into a change in phase shift (with time).

The rise and fall times of the proposed device have both been calculated to be 7 ps for a reverse a bias of 5 V, predicting an intrinsic bandwidth of several tens of gigahertz, although in practice large peak currents will probably reduce this slightly. This modulator provides improved performance in terms of loss and bandwidth compared to the strip waveguide device of Barrios and Lipson [33]. For a more detailed overview of the modulators in silicon photonics, see for example [34].

VI. Conclusion

The current trend in silicon photonics is to move to small waveguide dimensions, resulting in increased difficulty in maintaining single-mode operation, whilst simultaneously designing for polarization independence. However, it is possible to achieve such a design for small rib waveguides to the order of 1.0–1.5 μm in height. We have provided guidelines to aid such a design.

We have demonstrated a polarization independent design in ring resonators, where such behavior is particularly important. The intrinsic FSR of such devices is small due to the relatively large circumference of the ring resonators based on the rib waveguides, and it is for this reason that some other authors have moved to smaller devices fabricated in strip waveguides. However, we have demonstrated that it is possible to achieve respectable FSRs in polarization-independent rib waveguides, with a predicted FSR based on our existing results being as large as 12 nm, envisaging further improvement. We have also demonstrated an additional control of the quality factor of such devices via serial cascading of multiple rings.

However, we also have an interest in strip waveguides, and have reported both grating-based device designs and modulator designs in waveguides compatible with either strips or ribs. In particular, the modulators offer the potential of many tens of gigahertz modulation. In order to address the problem of coupling to very small waveguides, we have designed and fabricated a DGADC for coupling to very small waveguides, promising coupling efficiencies up to 90%, with 55% reported to date.

The question of whether to pursue polarization independence, however, remains complex. In particular, it is related to the application in question. For example, it is likely that for optimum modulation speed, a strip-waveguide-based modulator placed directly in front of a laser would not be required to exhibit polarization independence, because the laser is inherently polarized. Alternatively, a modulator fed via an optical fiber is much more likely to be required to satisfy polarization independent performance. Therefore, we can envisage systems in which the performance of some devices is considerably more critical than others, and hence, the question of whether to pursue polarization independence must be viewed from the perspective of the application in question. Fortunately, the flexibility of silicon photonics means there is room for both the approaches, and each approach has advantages in some application areas.

References

[1] R. A. Soref and J. P. Lorenzo, "All-silicon active and passive guided-wave components for $\lambda = 1.3$ and 1.6 μm," *IEEE J. Quantum Electron.*, vol. 22, no. 6, pp. 873–879, Jun. 1986.

[2] D. J. Albares and R. A. Soref, "Silicon-on-sapphire waveguides," in *Proc. SPIE Integr. Opt. Circuit Eng. IV*, 1987, vol. 704, pp. 24–25.

[3] B. L. Weiss, Z. Yang, and F. Namavar, "Wavelength dependent propagation loss characteristics of SiGe/Si planar waveguides," *Electron. Lett.*, vol. 28, pp. 2218–2220, 1992.

[4] E. Cortesi, F. Namavar, and R. A Soref, "Novel silicon-on-insulator structures for silicon waveguides," in *Proc. 1989 IEEE SOS/SOI Technol. Conf.*, Stateline, NV, Oct. 3–5, 1989, p. 109.

[5] F. Namavar, E. Cortesi, R. A. Soref, and P. Sioshansi, "On the formation of thick and multiple layer SIMOX structures and their applications," in *Proc. Ion Beam Process. Adv. Electron. Mater. Symp.,* San Diego, CA, Apr. 25–27, 1989.

[6] B. L. Weiss, G. T. Reed, S. K. Toh, R. A. Soref, and F. Namavar, "Optical waveguides in SIMOX structures," *IEEE Photon. Technol. Lett.*, vol. 3, no. 1, pp. 19–21, Jan. 1991.

[7] A. Rickman, G. T. Reed, B. L. Weiss, and F. Namavar, "Low-loss planar optical waveguides fabricated in SIMOX material," *IEEE Photon. Technol. Lett.*, vol. 4, no. 6, pp. 633–635, Jun. 1992.

[8] R. A. Soref and B. R. Bennett, "Kramers-Kronig analysis of electro-optical switching in silicon," in *Proc. SPIE Integr. Opt. Circuit Eng. IV*, Cambridge, MA, Sep. 16–17, 1986, vol. 704, pp. 32–37.

[9] C. K. Tang, G. T. Reed, A. J. Walton, and A G. Rickman, "Simulation of a low loss optical modulator for fabrication in SIMOX material," in *Proc. Silicon-Based Optoelectron. Mater. Symp.,* San Francisco, CA, Apr. 12–14, 1993.

[10] ——, "Low-loss, single-mode, optical phase modulator in SIMOX material," *J. Lightw. Technol.*, vol. 12, no. 8, pp. 1394–1400, Aug. 1994.

[11] C. K. Tang and G. T. Reed, "Highly efficient optical phase modulator in SOI waveguides," *Electron. Lett.*, vol. 31, pp. 451–452, 1995.

[12] G. T. Reed and A. P. Knights, *Silicon Photonics: An Introduction*. West Sussex, U.K.: Wiley, 2004.

[13] R. A. Soref, J. Schmidtchen, and K. Petermann, "Large single-mode rib waveguides in Ge-Si and Si-on-SiO_2," *IEEE J. Quantum Electron.*, vol. 27, no. 8, pp. 1971–1974, Aug. 1991.

[14] S. P. Pogossian, L. Vescan, and A. Vonsovici, "The single-mode condition for semiconductor rib waveguides with large cross section," *J. Lightw. Technol.*, vol. 16, no. 10, pp. 1851–1853, Oct. 1998.

[15] O. Powell, "Single-mode condition for silicon rib waveguides," *J. Lightw. Technol.*, vol. 20, no. 10, pp. 1851–1855, Oct. 2002.

[16] L. Vivien, S. Laval, B. Dumont, S. Lardenois, A. Koster, and E. Cassan, "Polarization-independent single-mode rib waveguides on silicon-on-insulator for telecommunication wavelengths," *Opt. Commun.*, vol. 210, pp. 43–49, 2002.

[17] J. Lousteau, D. Furniss, A. Seddon, T. M. Benson, A. Vukovic, and P. Sewell, "The single-mode condition for silicon-on-insulator optical rib waveguides with large cross section," *J. Lightw. Technol.*, vol. 22, no. 8, pp. 1923–1929, Aug. 2004.

[18] S. P. Chan, C. E. Png, S. T. Lim, V. M. N. Passaro, and G. T. Reed, "Single mode and polarization independent SOI waveguides with small cross section," *J. Lightw. Technol.*, vol. 23, pp. 1573–1582, 2005.

[19] S. P. Chan, V. M. N Passaro, and G. T. Reed, “Single mode condition and zero birefringence in small SOI waveguides,” *Electron. Lett.*, vol. 41, pp. 528–529, 2005.

[20] W. R. Headley, G. T. Reed, M. Paniccia, A. Liu, and S. Howe, “Polarization-independent optical racetrack resonators using rib waveguides on silicon-on-insulator,” *Appl. Phys. Lett.*, vol. 85, pp. 5523–5525, 2004.

[21] R. Baets, P. Dumon, W. Bogaerts, D. Thourhout, D. Taillaert, B. Luyssaert, P. Bienstman, V. Wiaux, S. Beckx, and J. Wouters, “Silicon-on-insulator platform for WDM components,” in *Proc. IEEE LEOS 17th Annu. Meeting*, Nov. 2004, vol. 2, pp. 741–742.

[22] Y. H. Ja, “A Vernier fiber double-ring resonator with a 3×3 fiber coupler and degenerate two-wave mixing,” *IEEE Photon. Technol. Lett.*, vol. 4, no. 5, pp. 1479–1485, 1995.

[23] T. W. Ang, G. T. Reed, A. Vonsovici, A. G. R. Evans, P. R. Routley, and M. R. Josey, “Effects of grating heights on highly efficient Unibond SOI waveguide grating couplers,” *IEEE Photon. Technol. Lett.*, vol. 12, no. 1, pp. 59–61, Jan. 2000.

[24] ——, “Highly efficient Unibond silicon-on-insulator blazed grating couplers,” *Appl. Phys. Lett.*, vol. 77, pp. 4214–4216, 2000.

[25] U. Bussmann, P. F. L. Hemment, A. K. Robinson, and V. V. Starkov, “Oxygen implantation through patterned masks: A method for forming insulated device islands while maintaining a planar wafer surface,” *Nucl. Instrum. Methods Phys. Res. B*, vol. 55, pp. 856–859, 1991.

[26] G. Z. Masanovic, V. M. N. Passaro, and G. T. Reed, “Dual grating-assisted directional coupling between fibers and thin semiconductor waveguides,” *IEEE Photon. Technol. Lett.*, vol. 15, no. 10, pp. 1395–1397, Oct. 2003.

[27] G. Z. Masanovic, G. T. Reed, W. Headley, B. Timotijevic, V. M. N. Passaro, R. Atta, G. Ensell, and A. G. R. Evans, “A high efficiency input/output coupler for small silicon photonic devices,” *Opt. Express*, vol. 13, pp. 7374–7379, 2005.

[28] L. Liao, D. Samara-Rubio, M. Morse, A. Liu, D. Hodge, D. Rubin, U. D. Keil, and T. Franck, “High speed silicon Mach–Zehnder modulator,” *Opt. Express*, vol. 13, pp. 3129–3135, 2005.

[29] C. E. Png, G. T. Reed, R. M. Atta, G. J. Ensell, and A. G. R. Evans, “Development of small silicon modulators in silicon-on-insulator (SOI),” in *Proc. SPIE*, vol. 4997, 2003, pp. 190–197.

[30] C. E. Png, S. P. Chan, S. T. Lim, and G. T. Reed, “Optical phase modulators for MHz and GHz modulation in silicon-On-insulator (SOI),” *J. Lightw. Technol.*, vol. 22, no. 6, pp. 1573–1583, Jun. 2004.

[31] Q. Xu, B. Shmidt, S. Pradhan, and M. Lipson, “Micrometre-scale silicon electro-optic modulator,” *Nature*, vol. 435, pp. 325–327, 2005.

[32] F. Y. Gardes, G. T. Reed, N. Emerson, and C. E. Png, “A sub micron depletion device, photonic modulator in silicon on insulator,” *Opt. Express*, vol. 13, pp. 8854–8854, 2005.

[33] C. A. Barrios and M. Lipson, “Modeling and analysis of high-speed electro-optic modulation in high confinement silicon waveguides using metal-oxide semiconductor configuration,” *J. Appl. Phys.*, vol. 96, pp. 6008–6015, 2004.

[34] G. T. Reed and C. E. Png, “Silicon optical modulators,” *Mater. Today*, vol. 8, pp. 40–50, 2005.

Graham T. Reed joined the University of Surrey, Guildford, U.K., in 1989, where he is currently leading an internationally recognized group. He has been associated with several companies and universities in the U.K., USA, France, Italy, Germany, Japan, and Singapore. His research interests include silicon integrated optical circuits, optical modulators, grating couplers, and optical sensing applications. He has authored or coauthored more than 150 publications in the field of guided-wave optoelectronics. He also coauthored the first textbook on silicon photonics, and is a holder of several patents.

Goran Z. Mashanovich received the Dipl. Ing. and M.Sc. degrees in electrical engineering from the Faculty of Electrical Engineering, University of Belgrade, Belgrade, Serbia, and the Ph.D. degree from the University of Surrey, Guildford, U.K.

He joined the Silicon Photonics Group in the School of Electronics and Physical Sciences, University of Surrey, in 2000, after working as a Teaching and Research Assistant with the Faculty of Electrical Engineering, University of Belgrade, for five years. His research interests include silicon photonics and fiber-optic sensors.

William R. Headley received the B.Sc. and M.Sc. degrees in physics from Purdue University, West Lafayette, IN, in 1997 and 2001, respectively. He received the Ph.D. degree in electronics engineering from the University of Surrey, Guildford, U.K., in 2005.

His research interests include integrated photonics for telecommunications devices, polarization effects in waveguides, and optical telecommunications networks in general.

Branislav Timotijevic was born in Serbia in 1978. He received the B.Sc. degree in electrical engineering from the Faculty of Electrical Engineering, University of Belgrade, Belgrade, Serbia, in 2002. He is currently working toward the Ph.D. degree at the Advanced Technology Institute, School of Electronics and Physical Sciences, University of Surrey, Guildford, U.K., under a scholarship from Intel Corporation.

His current research interests include optical filters in silicon-on-insulator and silicon photonics.

Mr. Timotijevic also received the Overseas Research Scholarship (ORS) Award in 2004.

Frederic Y. Gardes was born in France in 1977. He received the Diplôme Universitaire de Technologie (DUT) in physics measures from the Institut Universitaire de Technologie de Lannion, Lannion, France, in 1999, the B.Sc. degree (with honors) from the University of Portsmouth, Portsmouth, U.K., in 2001, and the M.Sc. degree in optoelectronics from the University of Northumbria, Newcastle, U.K., in 2002. He is currently working toward the Ph.D. degree at the Advanced Technology Institute, School of Electronics and Physical Sciences, University of Surrey, Guildford, U.K., under a scholarship from the Engineering and Physical Sciences Research Council (EPSRC).

His current research interests include integrated optics in silicon-on-insulator (SOI), numerical simulation of optical and semiconductor components, optical modulators based on the plasma dispersion effect, and ring resonators.

Seong Phun Chan was born in Malaysia in 1976. He received the B.Eng. (with honors) and Ph.D. degrees from the School of Electronics and Physical Sciences, University of Surrey, Guildford, U.K., in 2000 and 2005, respectively.

His research interests include integrated optics in silicon-on-insulator (SOI), numerical simulation of optical components, waveguide-based Bragg grating devices, and thermo-optic phenomena in SOI waveguides.

Peter Waugh was born in Kingston, U.K., in 1952. He received the Graduate degree in electronics from the University of Surrey, Guildford, U.K., in 1976. He received the Diploma in electronics and the Master’s degree in optical electronics. He is currently working toward the Ph.D. degree at the University of Surrey after retiring as Electronics Engineer in 2003.

Neil G. Emerson is currently a Senior Lecturer in the Department of Electronic Engineering at the University of Surrey, Guildford, U.K., and has been a member of the Surrey Centre for Research in Ion Beam Applications (SCRIBA) since he joined the university in 1984. He was formerly a Research Fellow at the Edinburgh Microfabrication Facility, University of Edinburgh, Edinburgh, U.K., where he was responsible for IC wafer process measurement and testing. He has authored many papers on a range of topics in the silicon/compound semiconductor field. His current research interests include ion beam synthesis of low-resistivity layers in amorphous silicon, electrically active defects and mechanical strain in Ge^+ implanted silicon, production of ultra-shallow layers in silicon, and developing a technology for producing future generation, sub-100-nm CMOS.

Ching Eng Png was born in Singapore in 1974. He received the B.Eng. degree (with honors) in electronic and electrical engineering and the Ph.D. degree from the University of Surrey, Guildford, U.K., in 1999 and 2004, respectively.

From November 1999 to September 2000, he was a Gigabit Optical Transceiver Engineer with Agilent Technologies, Singapore. He is currently with the Institute of High Performance Computing, Singapore, working on biophotonics and silicon photonics.

Dr. Png received the Royal Academy of Engineering Prize and the Institution of Electrical Engineers (IEE) Hudswell International Research Scholarship for his work on silicon optical modulators.

Mario J. Paniccia (M'04–A'04–SM'05) received the B.S. degree in physics from the State University of New York, Binghamton, in 1988, and the Ph.D. degree in solid-state physics from Purdue University, West Lafayette, IN, in 1994.

He is currently the Director of the Photonics Technology Laboratory at Intel Corporation, Santa Clara, CA, and directs a research group in the area of silicon photonics. He has been engaged in many areas of optical technologies during his career at Intel Corporation. His teams' pioneering activities in silicon photonics led to the development of the first silicon modulator with bandwidth$>$1 GHz in 2004, and the first continuous wave silicon laser in 2005. He has authored numerous papers, including three nature papers and two book chapters. He is the holder of over 61 issued or pending patents.

Ansheng Liu received the Ph.D. degree from the University of Aalborg, Aalborg, Denmark, in 1992.

He is currently a Research Scientist and Senior Staff Member at the Photonic Technology Laboratory, Intel Corporation, Santa Clara, CA, where he is developing silicon photonic devices in the Corporate Technology Group. Prior to joining Intel, in 2000, he was at the NASA Ames Research Center, the National Institute of Standards and Technology, and the University of Aalborg as an Assistant Professor. His current research interests include nonlinear optics of nanostructures, near-field optics, optoelectronics, and photonics.

Dani Hak was born in Israel in 1975. He received the B.Sc. degree in computer science and physics from the Hebrew University, Jerusalem, Israel, in 2003. He is currently working toward the M.Sc. degree in electrical engineering at Tel-Aviv University, Tel-Aviv, Israel.

Since 2002, he has been working on process development of silicon˜photonics devices at Intel Corporation, Jerusalem. His current research interests include waveguide-based detectors.

Vittorio M. N. Passaro (M'92–SM'05) was born in Bari, Italy, on November 23, 1962. He received the Laurea degree (*cum laude*) in electronic engineering from the University of Bari, Bari, Italy, in 1988, and the Ph.D. degree in electronic engineering, curriculum optoelectronics, in 1992.

Since October 2000, he has been an Associate Professor of electronic technologies at the Politecnico di Bari, Bari, Italy. His research interests include optoelectronic technologies, integrated optics, modeling, design, and simulation of a number of integrated optical devices and circuits for optical signal processing, telecommunications and sensor applications, dry etching, proton exchange technologies, and silicon photonics technology. He is the author or coauthor of more than 140 papers published in international journals and conference proceedings and holds two international patents.

Dr. Passaro is a member of the Optical Society of America (OSA).